Supplement of Biogeosciences, 20, 3895–3917, 2023
https://doi.org/10.5194/bg-20-3895-2023-supplement

Biogeosciences Open Access EGU

Supplement of

Modeling coupled nitrification–denitrification in soil with an organic hotspot

Jie Zhang et al.

Correspondence to: Jie Zhang (jiezh@agro.au.dk)

Supplement

S1. Initial conditions in the model

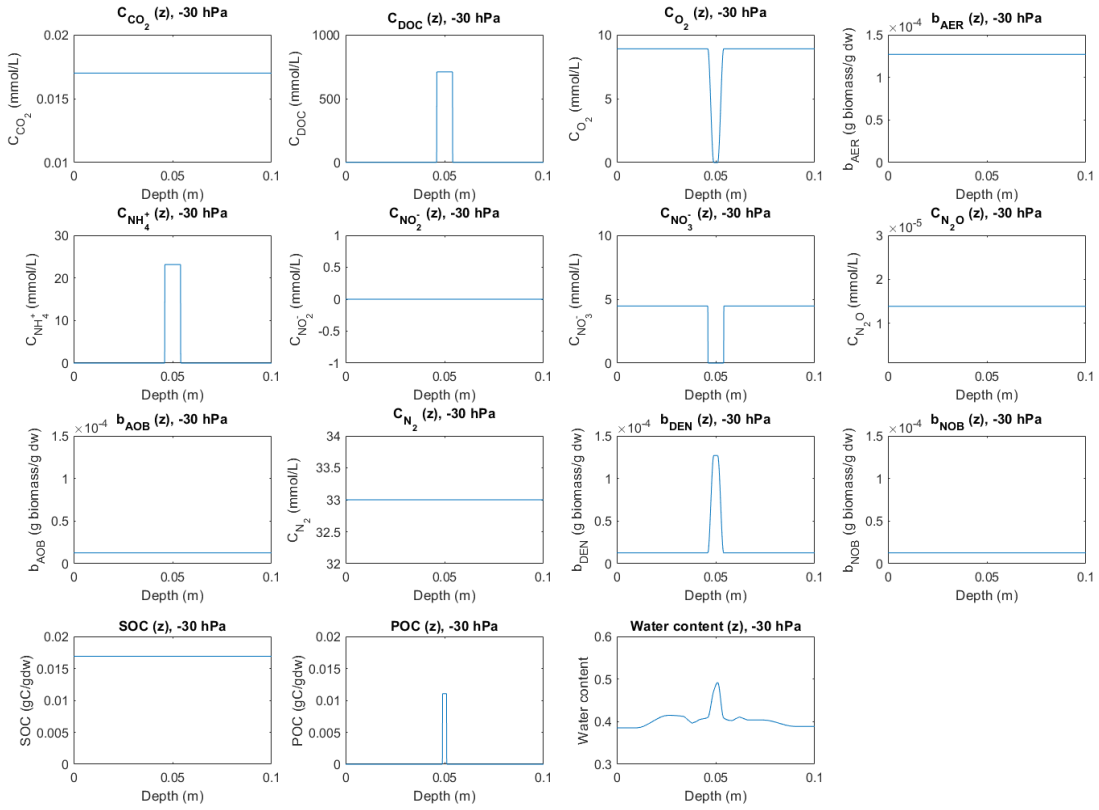

Figure S1. Initial values for non-uniformly distributed components and soil moisture in the -30 hPa treatment.

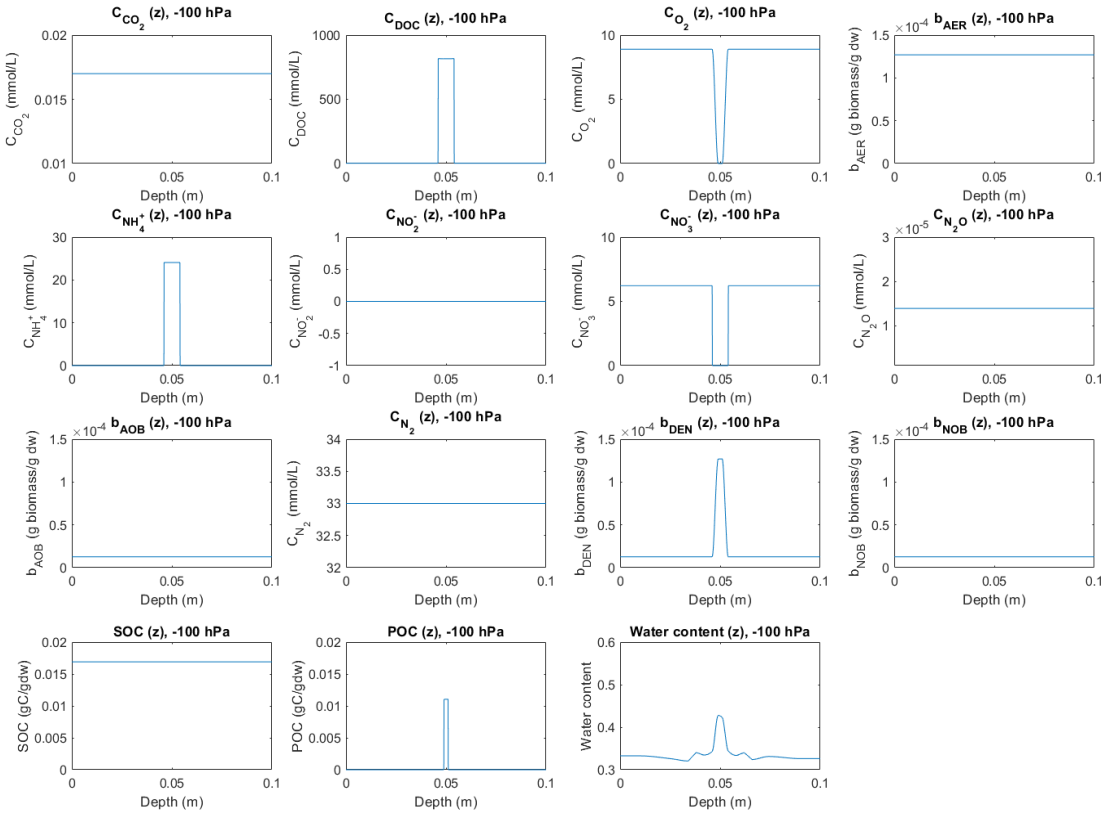

Figure S2. Initial values for non-uniformly distributed components and soil moisture in the -100 hPa treatment.

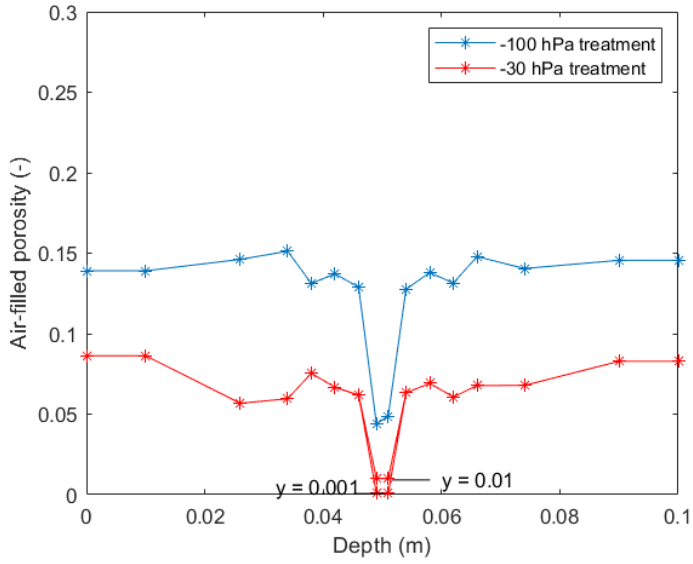

Figure S3. Air-filled porosity in the -30 hPa and -100 hPa treatments.

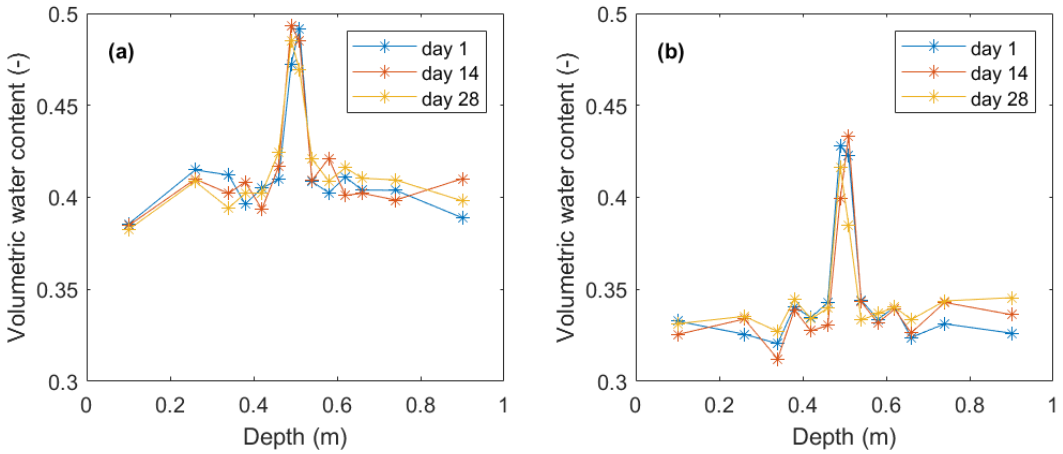

Figure S4. Volumetric water-filled porosity in (a) -30 hPa and (b) -100 hPa treatments.

S2. Simulated concentration profiles

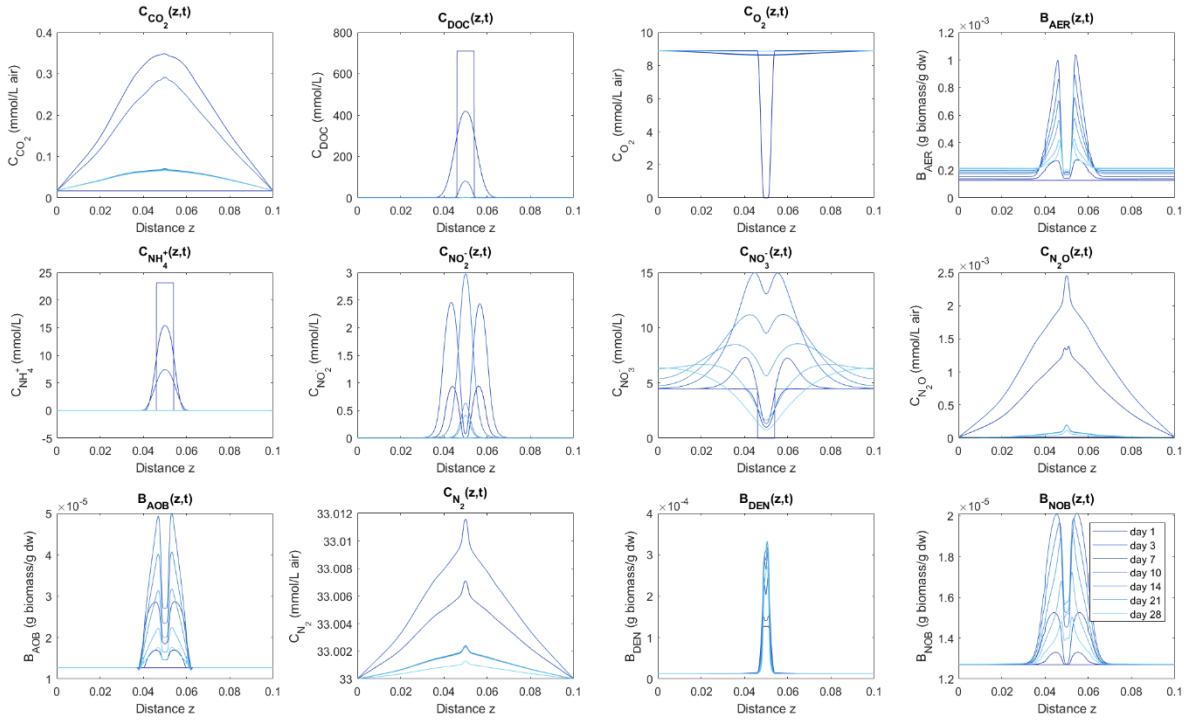

Figure S5. Simulated concentration profiles of 12 species numerically solved in the model for the -30 hPa treatment. Data are plotted on day 0, 1, 3, 7, 10, 14, 21, 28 where lighter colors indicates the increasing time.

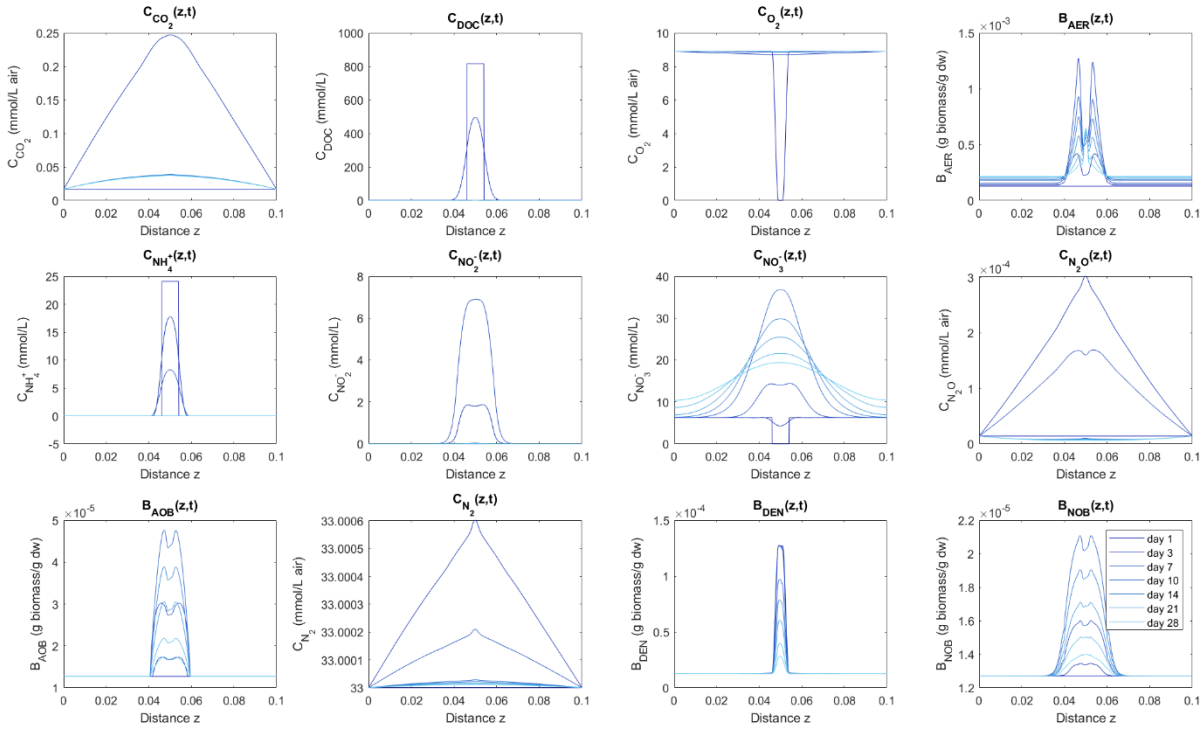

Figure S6. Simulated concentration profiles of 12 species numerically solved in the model for the -100 hPa treatment. Data are plotted on day 0, 1, 3, 7, 10, 14, 21, 28 where lighter colors indicates the increasing time.

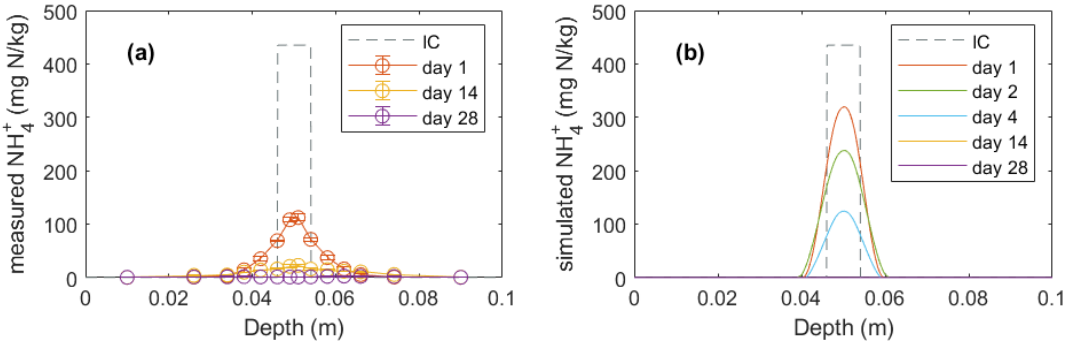

Figure S7. Measured and modeled NH_4^+ profiles in the -30 hPa treatment.

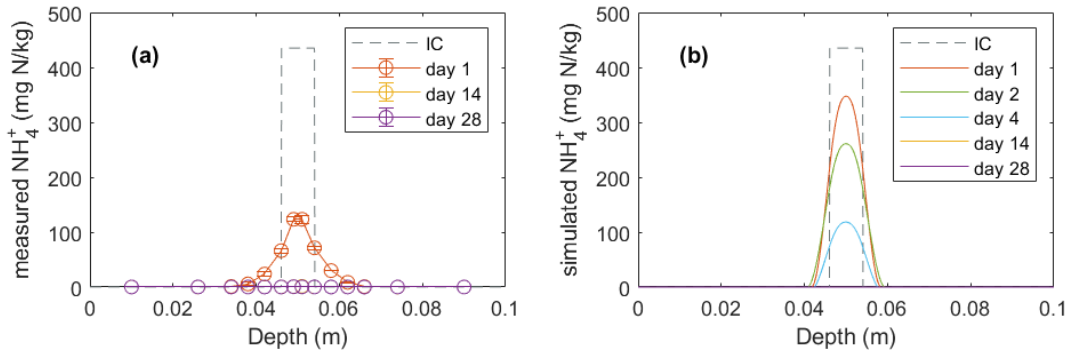

Figure S8. Measured and modeled NH_4^+ profiles in the -100 hPa treatment.

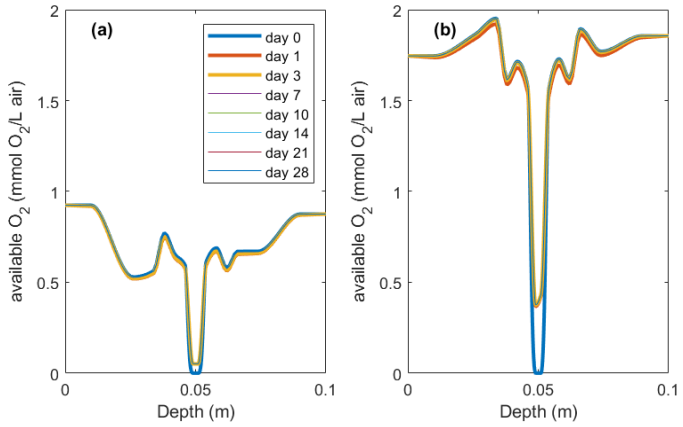

Figure S9. Simulated available O_2 content in model reactions in (a) -30 hPa and (b) -100 hPa treatments.

Table S1. Basic properties of the manure slurry. TOC was assumed to account for a fraction of 0.42 of VS (Petersen et al., 2016) and the fraction of DOC in TOC was 0.5, an intermediate estimate from two studies (Petersen et al., 1996, 2016).

Application rate ($kg\ fw/m^2$)	Volatile solids (g VS/kg fw)	TOC (g C/kg fw)	DOC (g C/kg fw)	POC (g C/kg fw)	NH_4^+ (g N/kg fw)	Dry matter (g/kg fw)
3.963	37.14	15.60	7.8	7.8	1.23	48.04

Table S2. Average measured values of soil samples taken at a distance of 1 cm from both surfaces in control treatments on day 1. SOC was estimated from LOI and the conversion model in (Jensen et al., 2018).

	LOI (g/100 g dw)	SOC (g/100 g dw)	NH_4^+ (mg N/kg dw)	NO_3^- (mg N/kg dw)

-30 hPa soil	5.09	1.69	0.090	17.86
-100 hPa soil	5.06	1.70	0.138	20.54

S3. Reactive and diffusional rates of N_2O, NO_2^-, CO_2, and O_2

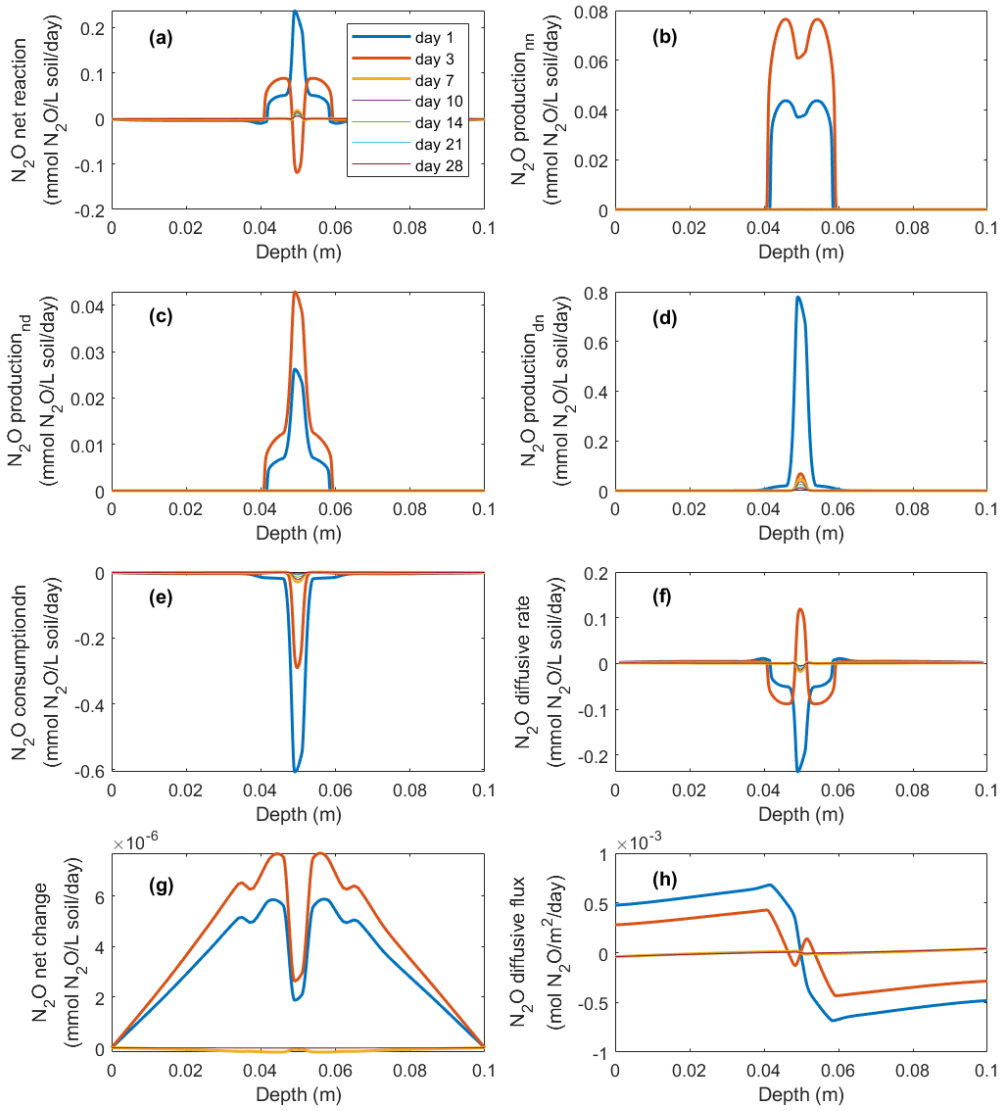

Figure S10. Simulated rates of N_2O production, consumption, and transport in the -100 hPa treatment: (a) net N_2O reaction rate, (b) N_2O production rate by nitrification, (c) N_2O production rate by nitrifier denitrification, (d) N_2O production rate by denitrification, (e) N_2O consumption rate by denitrification, (f) N_2O diffusive rate, (g) the net rate of N_2O changes by reactions and transport, and (h) N_2O diffusive flux, where the negative sign represents the

downward movement towards the lower soil-air interface (z = 0.1 m), and the positive sign the flow towards the upper soil-air interface (z = 0 m).

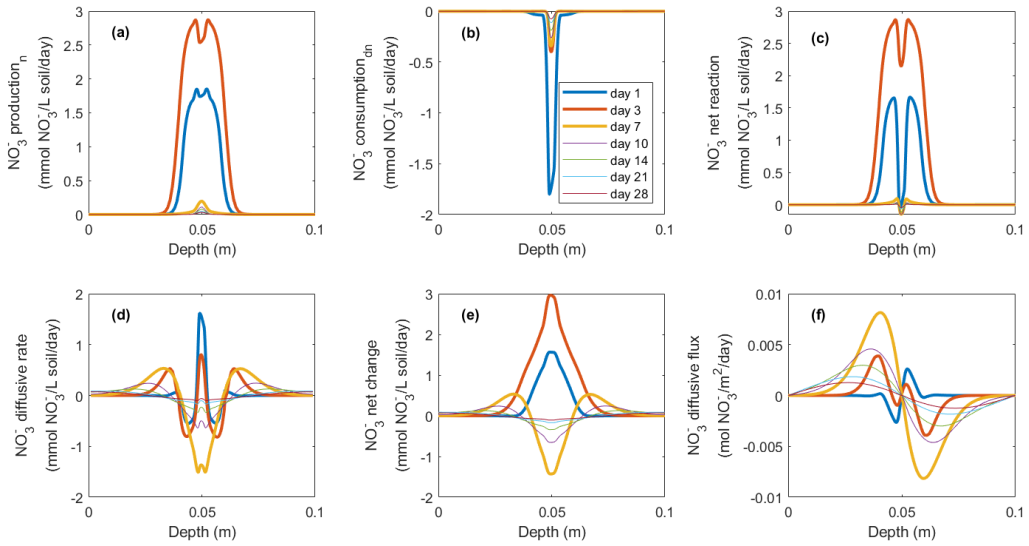

Figure S11. Simulated rates of NO_3^- production, consumption, and transport in the -100 hPa treatment: (a) NO_3^- production rate by nitrification; (b) NO_3^- consumption rate by denitrification; (c) net NO_3^- reaction rate; (d) NO_3^- diffusive rate; (e) the net rate of NO_3^- changes by reactions and transport; and (f) NO_3^- diffusive flux, where the negative sign represents the downward movement towards the lower soil-air interface (z = 0.1 m), and the positive sign the flow towards the upper soil-air interface (z = 0 m).

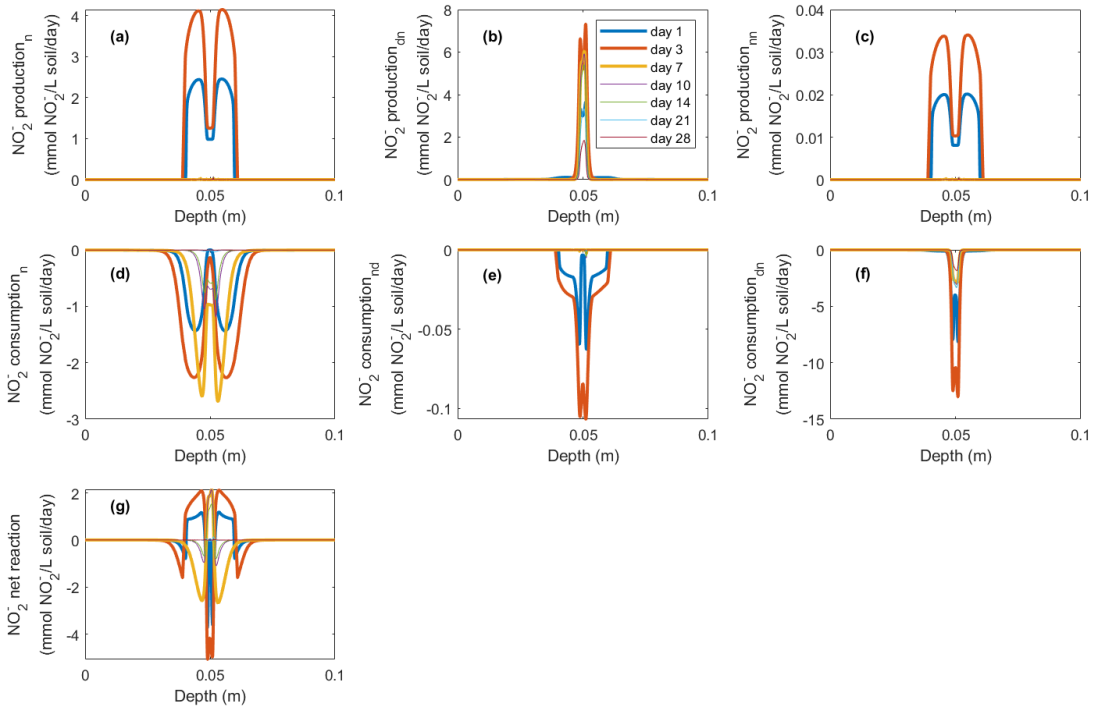

Figure S12. Simulated rates of NO_2^- production and consumption in the -30 hPa treatment: (a) NO_2^- production rate by nitrification; (b) NO_2^- production rate by denitrification; (c) NO_2^- production rate by nitrification (N_2O-production pathway); (d) NO_2^- consumption rate by nitrification; (e) NO_2^- consumption rate by nitrifier denitrification; (f) NO_2^- consumption rate by denitrification; and (g) net NO_2^- reaction rate.

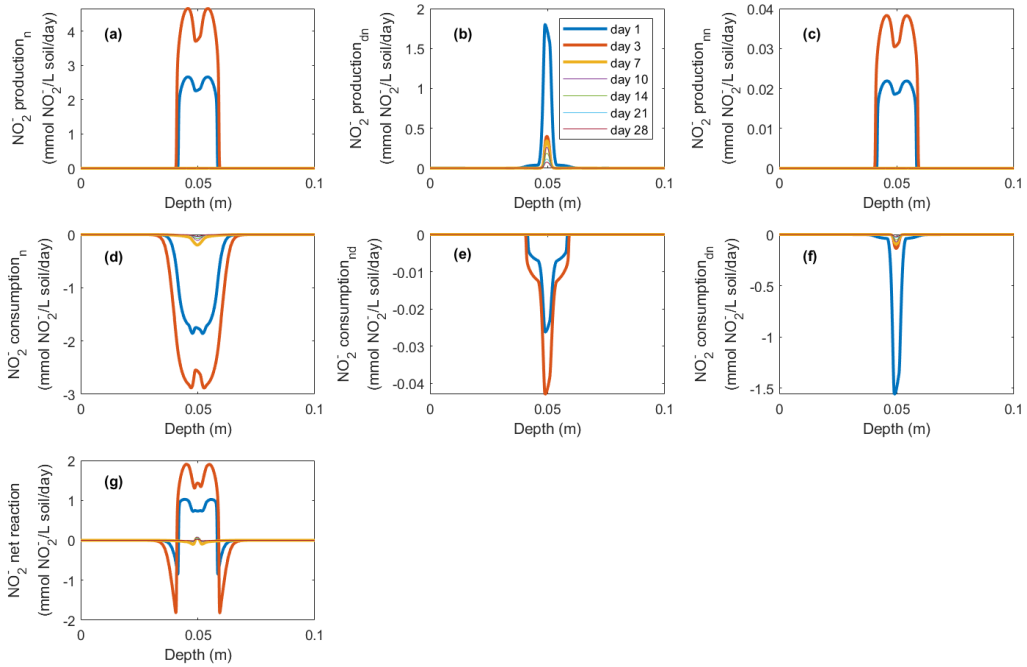

Figure S13. Simulated rates of NO_2^- production and consumption in the -100 hPa treatment: (a) NO_2^- production rate by nitrification; (b) NO_2^- production rate by denitrification; (c) NO_2^- production rate by nitrification (N_2O-

production pathway); (d) NO_2^- consumption rate by nitrification; (e) NO_2^- consumption rate by nitrifier denitrification; (f) NO_2^- consumption rate by denitrification; and (g) net NO_2^- reaction rate.

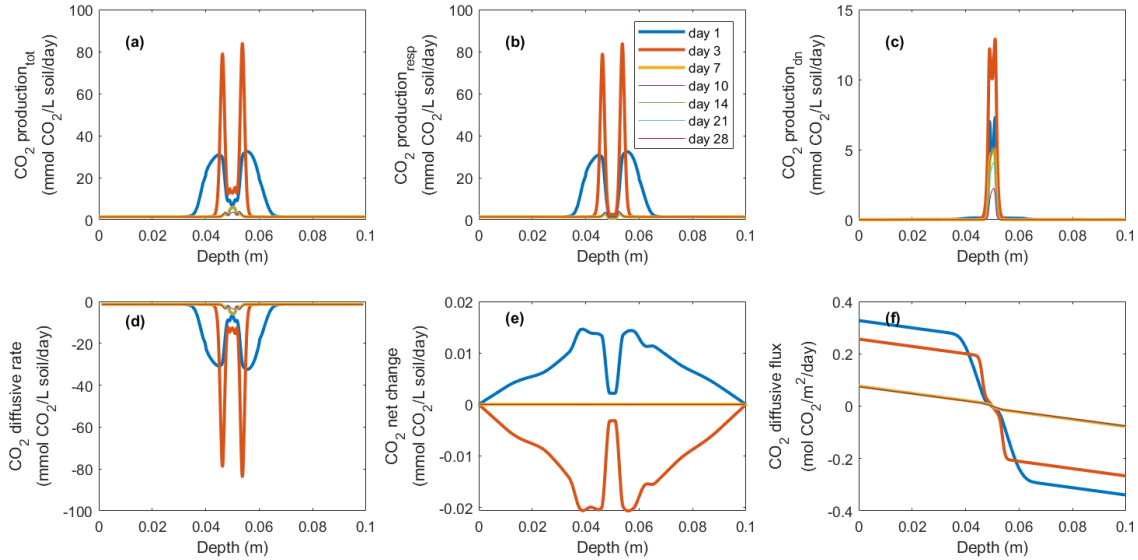

Figure S14. Simulated rates of CO_2 production, consumption, and transport in the -30 hPa treatment: (a) total CO_2 production rate; (b) CO_2 production rate by aerobic respiration; (c) CO_2 production rate by anaerobic respiration; (d) CO_2 diffusive rate; (e) the net rate of CO_2 changes by reactions and transport; and (f) CO_2 diffusive flux, where the negative sign represents the downward movement towards the lower soil-air interface (z = 0.1 m), and the positive sign the flow towards the upper soil-air interface (z = 0 m).

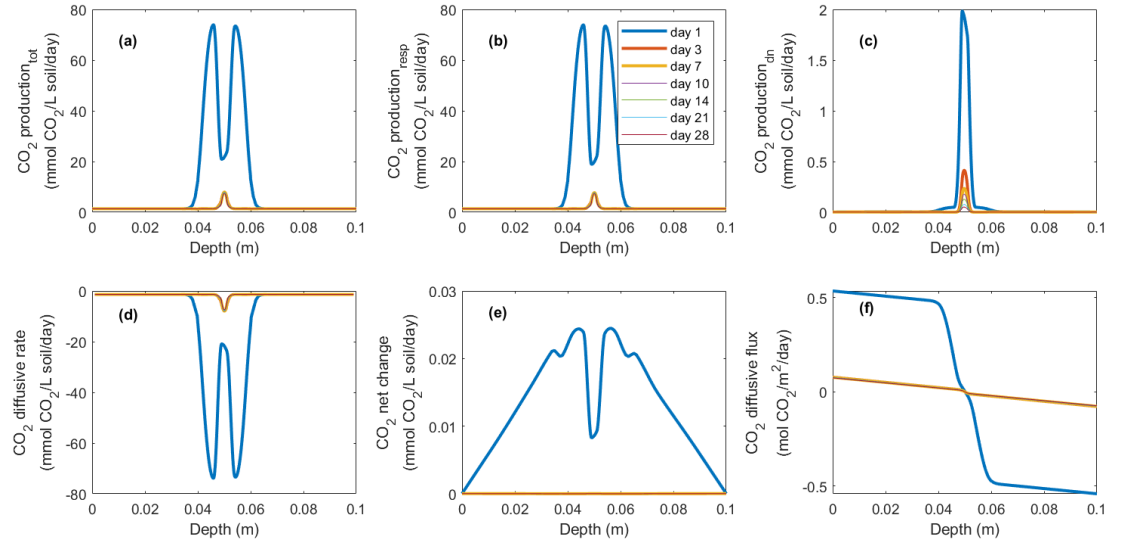

Figure S15. Simulated rates of CO_2 production, consumption, and transport in the -100 hPa treatment: (a) total CO_2 production rate; (b) CO_2 production rate by aerobic respiration; (c) CO_2 production rate by anaerobic respiration; (d) CO_2 diffusive rate; (e) the net rate of CO_2 changes by reactions and transport; and (f) CO_2 diffusive flux, where the negative sign represents the downward movement towards the lower soil-air interface (z = 0.1 m), and the positive sign the flow towards the upper soil-air interface (z = 0 m).

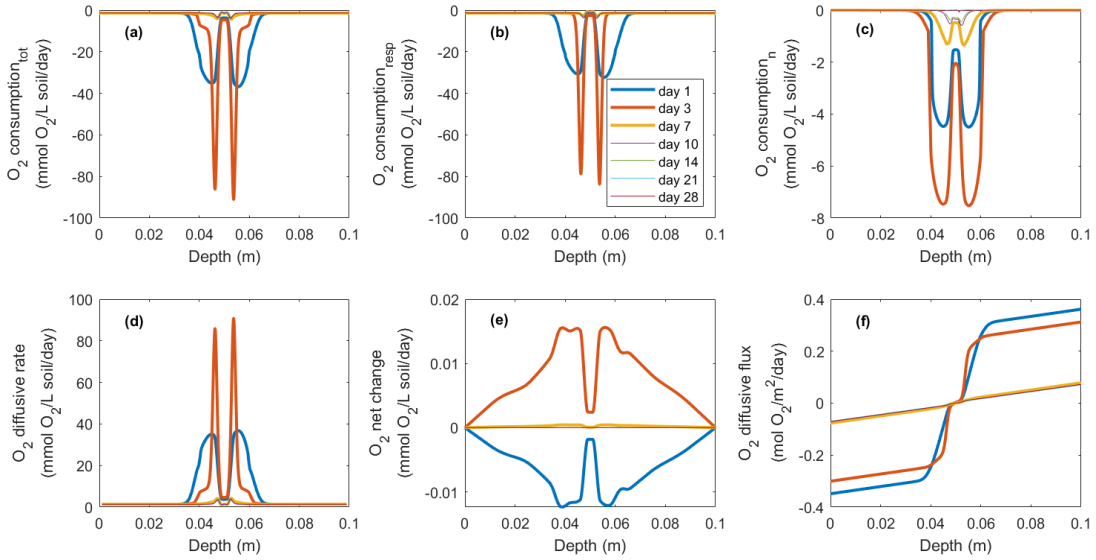

Figure S16. Simulated rates of O_2 production, consumption, and transport in the -30 hPa treatment: (a) total O_2 consumption rate; (b) O_2 consumption rate by aerobic respiration; (c) O_2 consumption rate by nitrification; (d) O_2 diffusive rate; (e) the net rate of O_2 changes by reactions and transport; and (f) O_2 diffusive flux, where the negative sign represents the downward movement towards the lower soil-air interface (z = 0.1 m), and the positive sign the flow towards the upper soil-air interface (z = 0 m).

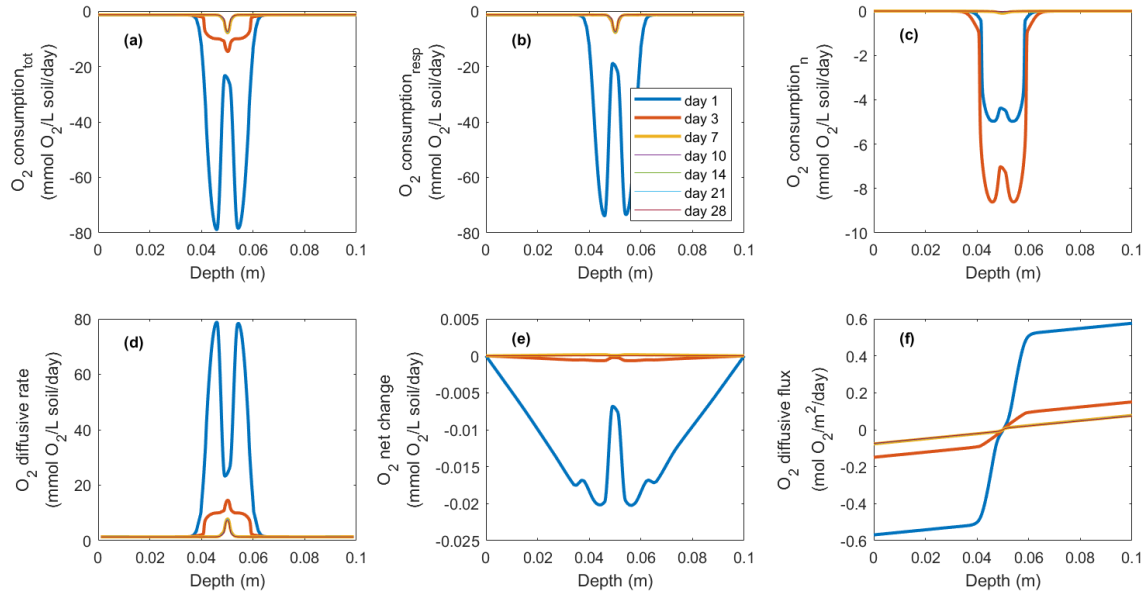

Figure S17. Simulated rates of O_2 production, consumption, and transport in the -100 hPa treatment: (a) total O_2 consumption rate; (b) O_2 consumption rate by aerobic respiration; (c) O_2 consumption rate by nitrification; (d) O_2 diffusive rate; (e) the net rate of O_2 changes by reactions and transport; and (f) O_2 diffusive flux, where the negative sign represents the downward movement towards the lower soil-air interface (z = 0.1 m), and the positive sign the flow towards the upper soil-air interface (z = 0 m).

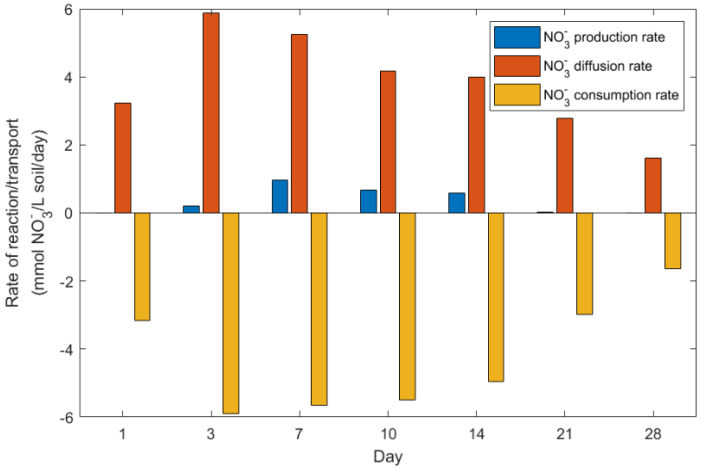

Figure S18. Average rates of NO_3^- production, diffusion, and consumption between 0.049-0.051 m in the simulation of the -30 hPa treatment.

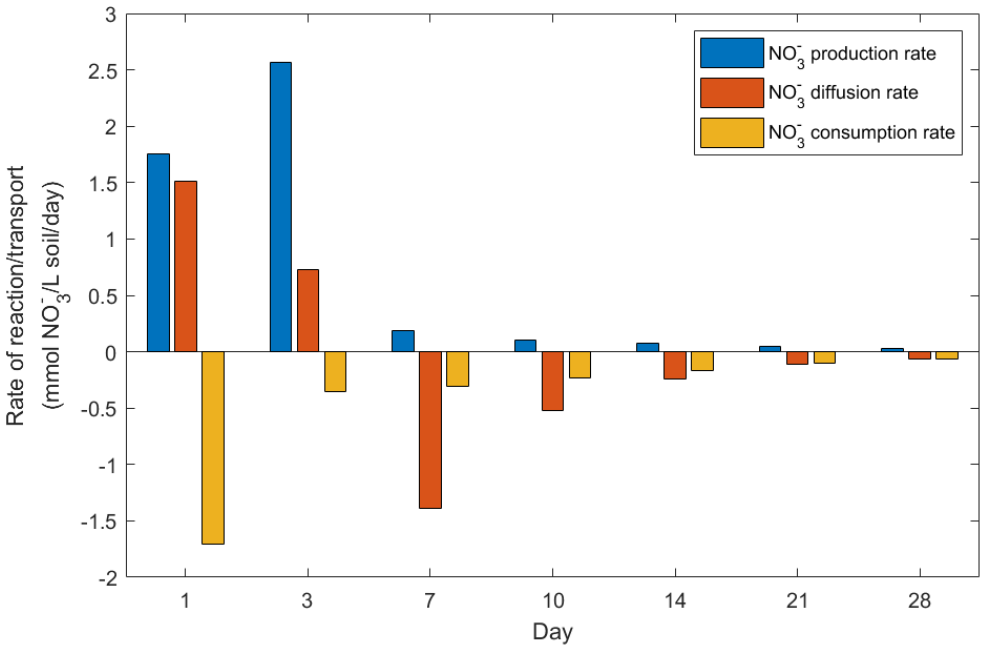

Figure S19. Average rates of NO_3^- production, diffusion, and consumption between 0.049-0.051 m in the simulation of the -100 hPa treatment.

S4. Scenario test: no solute diffusion

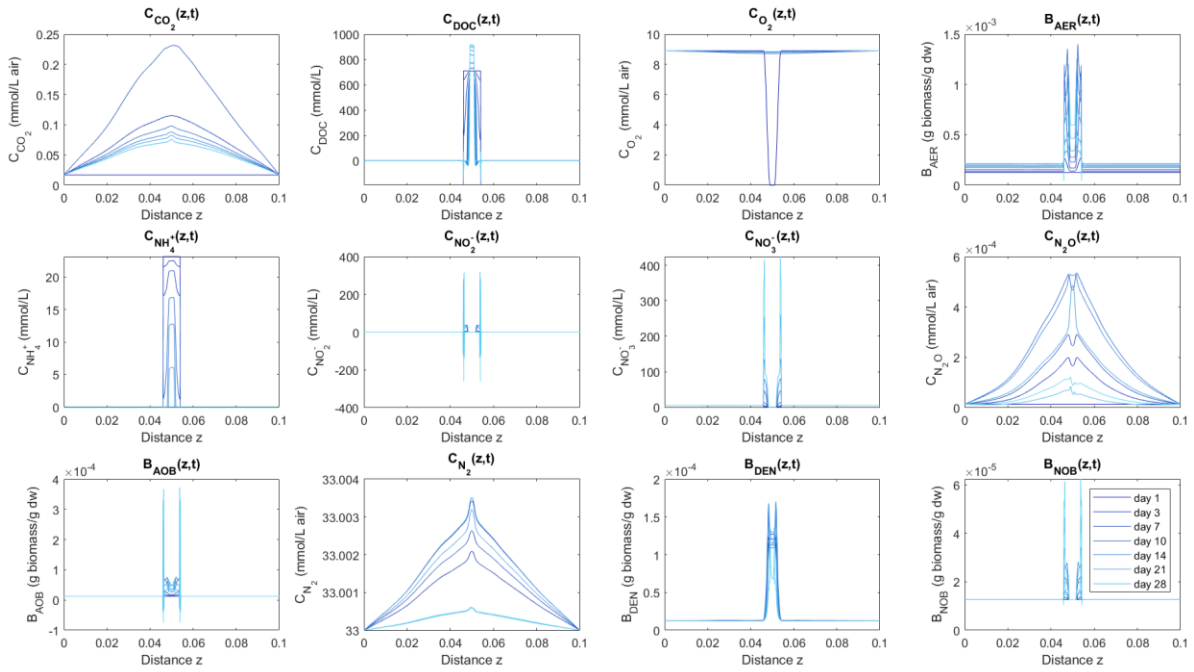

Figure S20. Simulated concentration profiles of 12 species numerically solved in the model for the -30 hPa treatment, without solute diffusion.

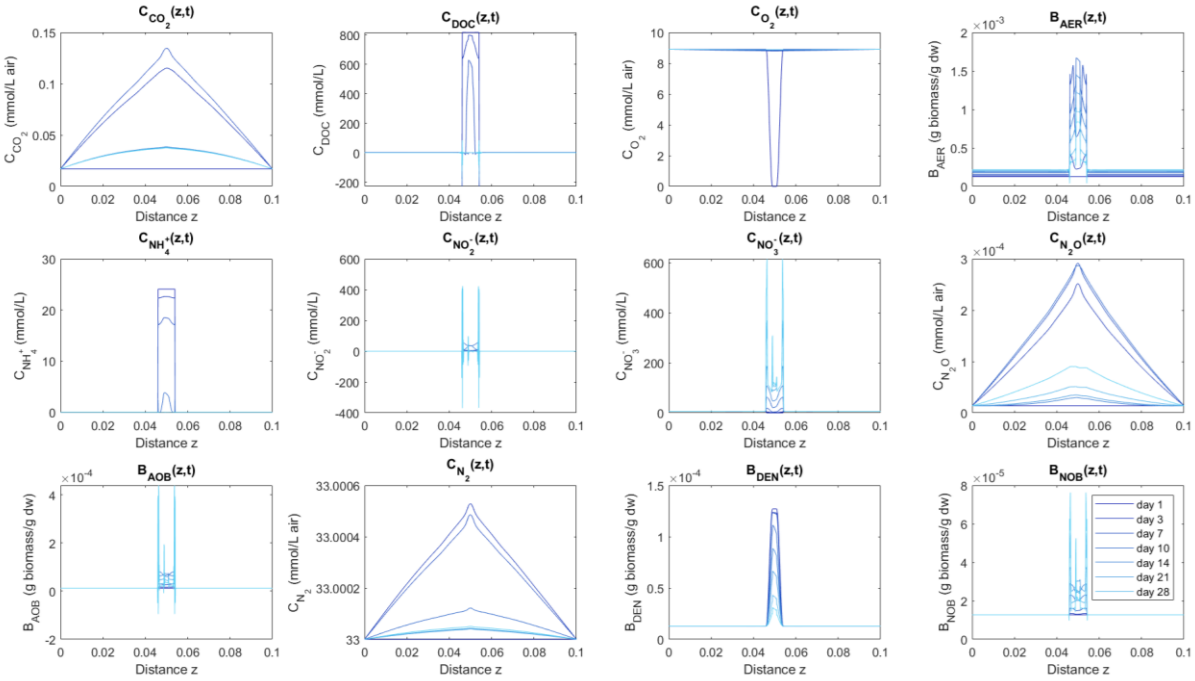

Figure S21. Simulated concentration profiles of 12 species numerically solved in the model for the -30 hPa treatment, without solute diffusion.

S5. Scenario test: change the small air fraction in the saturated zone

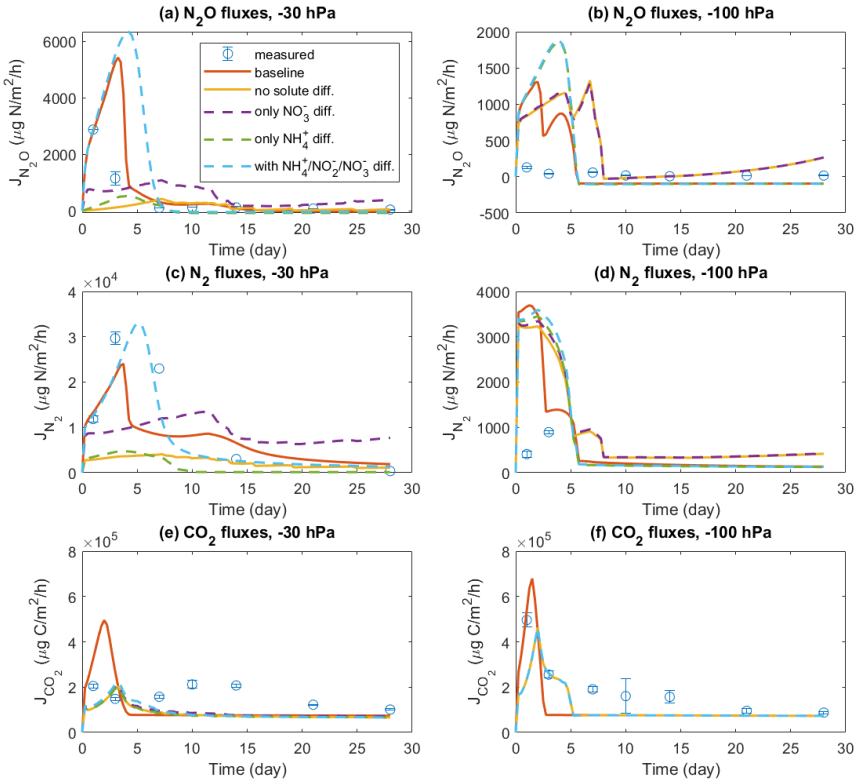

Figure S22. Comparison of different scenarios with respect to N_2O, N_2, and CO_2 fluxes in the -30 hPa and -100 hPa treatments. In each panel, there are measured data, a baseline simulation where the diffusion of all solutes is included, and four scenario 1~4, where Scenario 1 does not allow any solute diffusion, Scenario 2 allows only NO_3^- diffusion, Scenario 3 allows only NH_4^+ diffusion, and Scenario 4 allows diffusion of NH_4^+, NO_3^-, and NO_2^-, but not DOC. The small fraction of air porosity in the saturated zone in the -30 hPa treatment was set to 0.001.

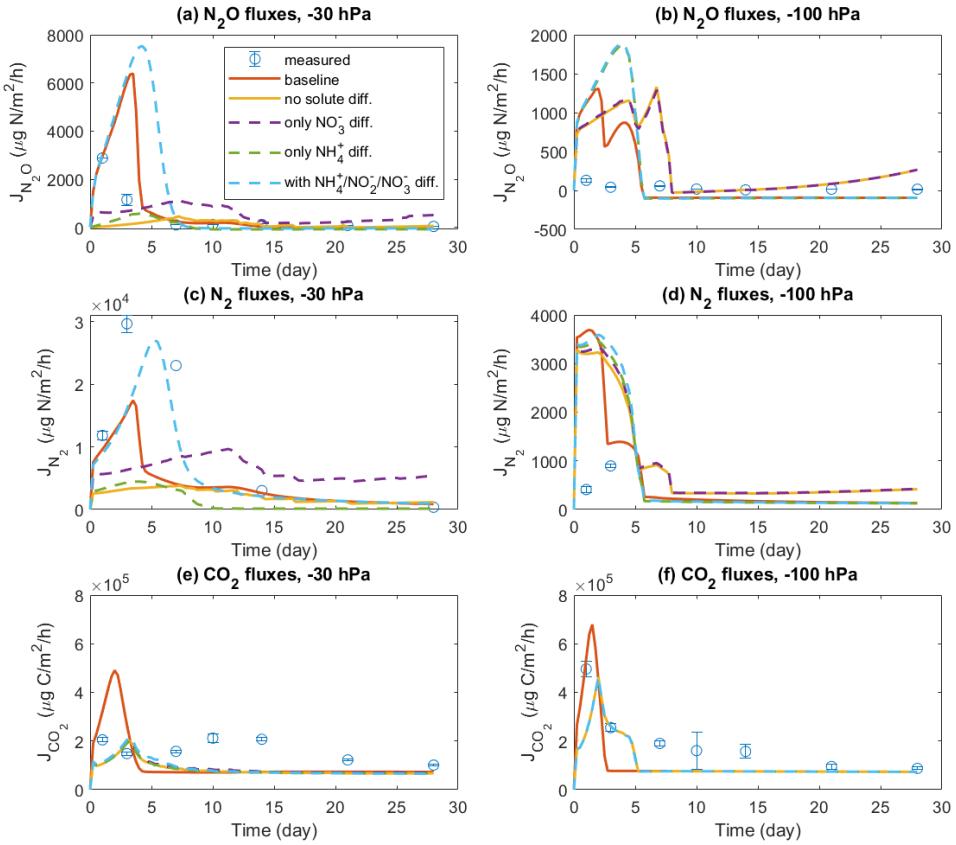

Figure S23. Comparison of different scenarios with respect to N_2O, N_2, and CO_2 fluxes in the -30 hPa and -100 hPa treatments. In each panel, there are measured data, a baseline simulation where the diffusion of all solutes is included, and four scenario 1~4, where Scenario 1 does not allow any solute diffusion, Scenario 2 allows only NO_3^- diffusion, Scenario 3 allows only NH_4^+ diffusion, and Scenario 4 allows diffusion of NH_4^+, NO_3^-, and NO_2^-, but not DOC. There was no small fraction of air porosity in the saturated zone in the -30 hPa treatment.

S6. Model implementation

S6.1 Calculating dissolved NH_4^+ concentration

In the measurement, the total mass of NH_4^+ in soil sample including the NH_4^+ dissolved in water and the NH_4^+ sorbed onto soil were extracted and measured. The mass concentration c_{tot} (mg/kg dw) was then obtained by dividing the total mass of NH_4^+ by the mass of dry soil. ρ_b and V indicate the bulk soil density and the volume of soil respectively.

$$c_{tot} = \frac{m_{\text{tot}}}{\text{mass of dry sample}} = \frac{m_{\text{tot}}}{\rho_b V} \tag{1}$$

The total mass of NH_4^+ in soil sample m_{tot} (mg) is the sum of NH_4^+ dissolved in water and NH_4^+ sorbed onto soil:

$$m_{tot} = m_s + m_w \tag{2}$$

The concentration of NH_4^+ sorbed in soil solids c_s (mg/kg dw) can be expressed in a Freundlich isotherm (Olesen et al., 1999):

$$c_s = K_F {c_w}^N \tag{3}$$

where c_w is the concentration of dissolved NH_4^+, K_F is the Freundlich distribution coefficient, and N is the dimensionless Freundlich isotherm exponent.

The mass of NH_4^+ sorbed in soil m_s is:

$$\begin{aligned} m_s &= c_s \rho_b V \\ &= K_F {c_w}^N \rho_b V \end{aligned} \tag{4}$$

The mass of NH_4^+ dissolved in water m_w is

$$m_w = c_w \theta_w V \tag{5}$$

where c_w is the concentration of dissolved NH_4^+ in soil water and θ_w is the soil water content.

The mass concentration c_{tot} obtained in the measurement is

$$\begin{aligned} c_{tot} &= \frac{m_{\text{s}} + m_{\text{w}}}{\rho_b V} \\ &= \frac{K_F {c_w}^N \rho_b V + c_w \theta_w V}{\rho_b V} \\ &= \frac{K_F {c_w}^N \rho_b + c_w \theta_w}{\rho_b} \end{aligned} \tag{6}$$

S6.2 Reaction processes

a. C mineralization

- Carbon mineralization under aerobic conditions is described by Eq. 1. C mineralization associated with denitrification is also represented in the model (see the following paragraphs).

$$CH_2O + O_2 \rightarrow CO_2 + H_2O \quad (7)$$

The rate of CO_2 generation, $S_{CO_2+,resp}$ (mmol CO_2/L soil/day) in the soil (note: we use the sign +/- following a component in the subscript to indicate the production/consumption of the component, and the same for the following section), in this equation can be written as:

$$S_{CO_2+,r} = \rho_b \mu_{CO_2,resp} B_{AER} \frac{[C]}{[C] + kM_{C-CO_2}} \times \frac{[O_2]}{[O_2] + kM_{O_2-CO_2}} \quad (8)$$

where $\mu_{CO_2,resp}$ (mmol CO_2 produced/g biomass/day) is the maximum reaction rate, and B_{AER} (unit: g biomass/g dw) is the microbial biomass responsible for aerobic respiration, and ρ_b (g dw/ L soil) is the bulk soil density. [C] (mmol C/L water) and [O_2] (mmol O_2/L air) represent available carbon and oxygen at the reactive sites of the enzyme, depending on the diffusion of solutes and gases within the soil medium.

$$[C_{aq}] = C_{aq} \times D_{aq} \times \theta_w^3 \quad (9)$$

$$[O_2] = O_2 \times D_g \times \theta_g^{4/3} \quad (10)$$

D_{aq} and D_g are unitless diffusion coefficients of solute in water and gas in air, respectively (Davidson et al., 2012). The value of D_{aq} is determined by assuming the extreme condition that $[C_{aq}] = C_{aq}$ for saturated soil, i.e. all of the soluble substrate is available at the reaction site under this condition. The value of D_{gas} is determined by another assumed extreme condition that all of the gas is available at the reaction site in completely dry soil. So, we have

$$D_{\mathrm{aq}} = f_{tot}^{-3} \quad (11)$$

$$D_{\mathrm{g}} = f_{tot}^{-4/3} \quad (12)$$

where f_{tot} is the total soil porosity.

The decomposition of soil organic matter (SOC, gC/g dw), and particulate organic matter in the manure (POC, gC/g dw), are described in first-order kinetics with the decay rate of α (1/day):

$$S_{SOC-} = \frac{\partial SOC(z,t)}{\partial t} = -\alpha_{SOC} SOC \quad (13)$$

$$S_{POC-} = \frac{\partial POC(z,t)}{\partial t} = -\alpha_{POC} POC \quad (14)$$

DOC production rates (S_{DOC+}, mmol C produced/L soil/day) from soil organic matter and particulate organic matter in the manure are expressed as:

$$S_{DOC+,SOC} = -\rho_b S_{SOC-} \times 10^3/12 \quad (15)$$

$$S_{DOC+,POC} = -\rho_b S_{POC-} \times 10^3/12 \quad (16)$$

Where DOC production rates are calculated from the decomposition rates of SOC and manure POC (g C/g dw/day) and bulk density ρ_b (g dw/ L soil), along with the g C to mol C conversion factor (1/12) and the mol to mmol conversion factor (10^3).

The total consumption rate of DOC by microbial intake and respiration was:

$$S_{DOC-,r} = -\frac{1}{1 - y_{AER}} S_{CO_2+,r} \quad (17)$$

where y_{AER} is the yield coefficient of aerobic heterotrophs.

b. Nitrification and nitrifier denitrification

Nitrification is the oxidation of NH_4^+ to NO_3^- via NO_2^- by autotrophs.

Nitrification:

$$\mathrm{NH_4^+ + 1.5O_2 \rightarrow NO_2^- + 2H^+ + H_2O} \quad (18)$$

$$\mathrm{NO_2^- + 0.5O_2 \rightarrow NO_3^-} \quad (19)$$

$$\mathrm{2.5NH_4^+ + 2.75O_2 \rightarrow N_2O + 0.5NO_2^- + 3H^+ + 3.5H_2O} \quad (20)$$

Nitrifier denitrification:

$$\mathrm{NO_2^- + NH_4^+ + 0.5O_2 \rightarrow N_2O + 2H_2O} \quad (21)$$

Oxygen consumption by nitrifiers is included in these steps. The rate of NO_2^- production, and NO_3^- production depends on the availability of parent substrates and O_2:

$$S_{NO_2^-+,nn} = \rho_b \mu_{NO_2^-,nn} B_{AOB} \frac{[NH_4]}{[NH_4] + kM_{NH_4-NO_2}} \times \frac{[O_2]}{[O_2] + kM_{O_2-NO_2}} \quad (22)$$

$$S_{NO_3^-+,nn} = \rho_b \mu_{NO_3^-,nn} B_{AOB} \frac{[NO_2^-]}{[NO_2^-] + kM_{NO_2-NO_3}} \times \frac{[O_2]}{[O_2] + kM_{O_2-NO_3}} \quad (23)$$

N_2O production from nitrification,

$$S_{N_2O+,nn} = \rho_b \mu_{N_2O+,nn} B_{AOB} \frac{[NH_4]}{[NH_4] + kM_{NH_4-N_2O}} \times \frac{[O_2]}{[O_2] + kM_{O_2-N_2O,nn}} \quad (24)$$

N_2O production from nitrifier denitrification,

$$S_{N_2O+,nd} = \rho_b \mu_{N_2O+,nd} B_{AOB} \frac{[NO_2^-]}{[NO_2^-] + kM_{NO_2-N_2O}} \frac{[NH_4]}{[NH_4] + kM_{NH_4-N_2O}} \times \frac{[O_2]}{[O_2] + kM_{O_2-N_2O,nd}} \times \frac{kI_{N_2O}}{[O_2] + kI_{N_2O,nd}} \quad (25)$$

The total rate of NH_4^+ consumption for chemical reaction and ammonia oxidizing bacteria (AOB) growth,

$$S_{NH_4^+-,n} = -\frac{1}{1-y_{AOB}}(S_{NO_2^-+,nn} + 2.5S_{N_2O+,nn} + S_{N_2O+,nd}) \tag{26}$$

where y_{AOB} is the yield coefficient of AOB.

The rate of NO_2^- consumption for producing NO_3^- and nitrite oxidizing bacteria (NOB) growth:

$$S_{NO_2^--,n} = -\frac{1}{1-y_{NOB}}S_{NO_3^-+,n} \tag{27}$$

where y_{NOB} is the yield coefficient of NOB.

O_2 consumption can be calculated by the production rates of nitrogen oxides in the nitrification process:

$$S_{O_2-,n} = -(1.5S_{NO_2^-+,n} + 0.5S_{NO_3^-+,n} + 2.75S_{N_2O+,nn} + 0.5S_{N_2O+,nd}) \tag{28}$$

c. Denitrification

In the present model, the considered pathways of stepwise denitrification include:

$$NO_3^- + 0.5CH_2O \rightarrow NO_2^- + 0.5CO_2 + 0.5H_2O \tag{29}$$

$$2NO_2^- + CH_2O + 2H^+ \rightarrow N_2O + CO_2 + 2H_2O \tag{30}$$

$$N_2O + 0.5CH_2O \rightarrow N_2 + 0.5CO_2 + 0.5H_2O \tag{31}$$

The rates of generation for denitrification products NO2-, N2O and N2, as well as CO2, are written as follows:

$$S_{NO_2^-+,dn} = \rho_b \mu_{NO_2^-,dn} B_{dn} \frac{[NO_3^-]}{[NO_3^-] + kM_{NO_3^- - NO_2^-}} \times \frac{[C]}{[C] + kM_{C-NO_2^-}} \times \frac{kI_{NO_2^-}}{[O_2] + kI_{NO_2^-,dn}} \tag{32}$$

$$S_{N_2O+,dn} = \rho_b \mu_{N_2O,dn} B_{dn} \frac{[NO_2^-]}{[NO_2^-] + kM_{NO_3 - N_2O}} \times \frac{[C]}{[C] + kM_{C-N_2O}} \times \frac{kI_{N_2O}}{[O_2] + kI_{N_2O,dn}} \tag{33}$$

$$S_{N_2+,dn} = \rho_b \mu_{N_2,dn} B_{dn} \frac{[N_2O]}{[N_2O] + kM_{N_2O}} \times \frac{[C]}{[C] + kM_{C-N_2}} \times \frac{kI_{N_2}}{[O_2] + kI_{N_2,dn}} \tag{34}$$

$$S_{CO_2+,dn} = 0.5S_{NO_2^-+,dn} + S_{N_2O+,dn} + 0.5S_{N_2+,dn} \tag{35}$$

The total consumption rate of DOC in denitrification including denitrifier (DEN) growth:

$$S_{DOC-,dn} = -\frac{1}{1-y_{DEN}}S_{CO_2+,dn} \tag{36}$$

where y_{DEN} is the yield coefficient of denitrifiers.

Given the process reactions, the net rate of change in Eq. (1) of the components listed can be written as follows:

$$\sum S_{DOC} = -\frac{1}{1-y_{AER}}S_{CO_2+,r} - \frac{1}{1-y_{DEN}}S_{CO_2+,dn} + S_{DOC+,SOC} + S_{DOC+,POC} \tag{37}$$

$$\sum S_{CO_2} = S_{CO_2+,r} + S_{CO_2+,dn} \quad (38)$$

$$\sum S_{NO_3^-} = S_{NO_3^-+,n} - S_{NO_2^-+,dn} \quad (39)$$

$$\sum S_{NO_2^-} = S_{NO_2^-+,n} + S_{NO_2^-+,dn} + 0.5S_{N_2O+,nn} - \frac{1}{1-y_{NOB}} S_{NO_3^-+,n} - S_{N_2O+,nd} - 2S_{N_2O+,dn} \quad (40)$$

$$\sum S_{NH_4^+} = -\frac{1}{1-y_{AOB}} (S_{NO_2^-+,n} + 2.5S_{N_2O+,nn} + S_{N_2O+,nd}) \quad (41)$$

$$\sum S_{N_2O} = S_{N_2O+,nn} + S_{N_2O+,nd} + S_{N_2O+,dn} - S_{N_2+,dn} \quad (42)$$

$$\sum S_{N_2} = S_{N_2+,dn} \quad (43)$$

$$\sum S_{O_2} = -(S_{CO_2+,r} + 1.5S_{NO_2^-+,n} + 0.5S_{NO_3^-+,n} + 2.75S_{N_2O+,nn} + 0.5S_{N_2O+,nd}) \quad (44)$$

Kinetic control of microbial biomass, including nitrifying bacteria and denitrifying bacteria, is described by the Monod equations:

$$\frac{d[B_{AER}]}{dt} = -y_{AER}/f_{Cbio}S_{DOC-,r} \times 10^{-3} \times 12/\rho_b - a_{AER}B_{AER} \quad (45)$$

$$\frac{d[B_{AOB}]}{dt} = -y_{AOB}/f_{Nbio}S_{NH_4^+-,n} \times 10^{-3} \times 14/\rho_b - a_{AOB}B_{AOB} \quad (46)$$

$$\frac{d[B_{NOB}]}{dt} = -y_{NOB}/f_{Nbio}S_{NO_2^--,n} \times 10^{-3} \times 14/\rho_b - a_{NOB}B_{NOB} \quad (47)$$

$$\frac{d[B_{DEN}]}{dt} = -y_{DEN}/f_{Cbio}S_{DOC-,dn} \times 10^{-3} \times 12/\rho_b - a_{DEN}B_{DEN} \quad (48)$$

Where the bacterial growth rates ($\frac{d[B_{pr}]}{dt}$, g biomass/g dw/day) are assumed to be proportional to the consumption rates of substrates ($S_{substrate-,pr}$, mmol C or N/L soil/day), linked by the bulk soil density (ρ_b, g dw/ L soil), yield coefficients (y_{pr}, g C/g C or g N/g N), and C or N content in microbial biomass (f_{Cbio}, f_{Nbio}), along with the mmol to mol conversion factor (10^{-3}), the mol C to g C conversion factor (12), and the mol N to g N conversion factor (14).

S6.3 Initial conditions

a. Dissolved organic carbon (DOC)

- Manure

Manure application rate in the soil core was 3963 g fw/m^2 (39.63 t/ha). Volatile solids in the cattle slurry used in the experiment was 37.14 g VS/kg fw, and by assuming total organic carbon (TOC) accounted for a fraction of 0.42 of

VS (Petersen et al., 2016), the amount of TOC in the applied manure was 61.82 g C/m^2. We assumed that the fraction of DOC in TOC was 0.5, an intermediate estimate from two studies (Petersen et al., 1996, 2016), and hence the amount of DOC was 30.91 g C/m^2. We assumed that at the starting point of reactions, manure DOC were concentrated in the zone of manure-saturated zone, i.e. ca. 4 mm from the center to each side (a length of ca. 8 mm), with a constant concentration.

$$C_{DOC,m} = \frac{f_{DOC,m} M_{TOC,m}}{12 \int_{z1}^{z2} \theta dz} \quad (49)$$

where $C_{DOC,m}$ (mol/m^3 or mmol/L) is the concentration of manure DOC, $M_{TOC,m}$ is the amount of manure TOC in application (g C/m^2), $f_{DOC,m}$ is the conversion factor (0.5) from manure TOC to DOC, 1/12 is the conversion factor from g C to mol C, and z_1 and z_2 are the locations of the initial manure DOC zone (z_1= 0.046 m, z_2= 0.054 m). The dissolved organic carbon from manure, $C_{DOC,m}(z)$ is a discretized function over depth, where the value is zero for $z<z_1$ and $z>z_2$ and non-zero for $z_1<z<z_2$.

- Soil

We took the average LOI value at 0.01 m and 0.09 m in the control soil core by day 1 as the initial LOI value for the manure treatment. Initial SOC values were estimated from the regression relationship SOC = 0.39LOI – 0.28 (Jensen et al., 2018), which were 0.0169 g C/g dw and 0.0170 g C/g dw for -100 hPa and -30 hPa treatments, respectively. The simulated scenarios represents spring conditions, and it appears that DOC concentrations in the Foulum soil are fairly constant at this time (one year after grassland cultivation) at 20-25 mg C/L (Gjettermann et al., 2008). A conversion factor of 3.5×10^{-4} was estimated as the ratio between dissolved organic C and total soil C for Foulum loamy sand soil so that the estimated DOC concentration became consistent with the reported range. The DOC concentration in the soil was calculated as:

$$C_{DOC,s} = \frac{f_{DOC,s} M_{SOC,s} 10^3 \rho_b}{12\theta(z)} \quad (50)$$

Where $C_{DOC,s}$ is the DOC concentration (mmol C/L), $M_{SOC,s}$ is the SOC content (g C/g dw), $f_{DOC,m}$ is the conversion factor (3.5×10^{-4}) from SOC to DOC, ρ_b is the bulk density (g dw/L soil) along with the conversion factor 10^3 from (g dw/L soil) to (g dw/m^3 soil), 1/12 is the conversion factor from g C to mol C, and $\theta(z)$ is the volumetric water content at depth *z*.

The initial DOC value within the soil was the sum of manure DOC ($C_{DOC,m}$) and soil DOC ($C_{DOC,s}$) as determined by treatment.

b. NH_4^+

- Manure

NH_4^+ content in the manure was 1.23×10^{-3} g N/g fw, and with an application rate of 3963 g fw/m^2, the amount of applied NH_4^+ was 4.87 g N/m^2. Similar to manure DOC, we assumed that the initial manure NH_4^+ input for model

simulation was concentrated in the zone of manure liquid, ca. 4 mm from the center to each side, with a constant concentration.

$$C_{NH4,m} = \frac{M_{NH4,m}}{10^3 \rho_b (z_2 - z_1)} \times \frac{18}{14} \times 10^6 \quad (51)$$

where $C_{NH4,m}$ is NH_4^+ content per dry weight (mg NH_4^+/kg dw), $M_{NH4,m}$ is the amount of manure NH_4^+ in application (g N/m^2), ρ_b is the bulk density (g dw/L soil) along with the conversion factor 10^3 from (g dw/L soil) to (g dw/m^3 soil), and $(z_2 - z_1)$ is the length of the initial manure NH_4^+ zone (m). We use the dissolved NH_4^+ content instead of NH_4^+-N in the following calculation, so a factor $\frac{18}{14} * 10^6$ was used to convert (g N/g dw) to (mg NH_4^+/kg dw).

The concentration of dissolved NH_4^+ within the manure-concentrated zone was calculated from the Freundlich model (Eq. 6) and the average water content within the initial NH_4^+ zone as follows,

$$C_{NH4,m,aq} = \frac{C_{NH4,m} \rho_b}{K_F C_{NH4,m,aq}^{N-1} \rho_b + \theta_{z1,z2}} \quad (52)$$

where $C_{NH4,aq}$ is the dissolved NH_4^+ content (mg NH_4^+/L), $C_{NH4,m}$ is the total NH_4^+ content (mg NH_4^+/kg dw), ρ_b is the bulk density (kg dw/L soil), K_F is the Freundlich distribution coefficient 4.89, and N is the dimensionless Freundlich isotherm exponent 0.74, adopting the sorption properties of a loamy sand soil in (Olesen et al., 1999). $\theta_{z1,z2}$ is the average water content within the initial NH_4^+ zone. The molar concentration of NH_4^+-N was calculated by dividing $C_{NH4,aq}$ by 18. The dissolved NH_4^+ from manure, $C_{NH4,m(aq)}(z)$ is a discretized function over depth, where the value is zero for $z<z_1$ and $z>z_2$ and non-zero for $z_1<z<z_2$.

- Soil

The initial NH_4^+ content of the bulk soil in the manure treatment was approximated by the measurements of control treatments at day 1. We took the average values of NH_4^+ content at the depths of 0.01 m and 0.09 m in the control as the initial values of soil NH_4^+, which were 0.138 mg N/kg and 0.090 mg N/kg for the -100 hPa and -30 hPa treatments respectively. The dissolved soil NH_4^+ content was calculated in the same way as the manure NH_4^+ with consideration of the volumetric water profile $\theta(z)$. The initial dissolved NH_4^+ within the soil core was the sum of dissolved NH_4^+ from manure and from soil.

c. NO_3^-

Similar to the calculation of initial DOC and NH_4^+, we used the average values of NO_3^- content at the depths of 0.01 m and 0.09 m in the control from day 1 as the initial values of soil NO_3^-. They were 20.54 mg N/kg and 17.86 mg N/kg for the -100 hPa and -30 hPa treatments respectively. We assumed that the soil pore water in the middle of soil core was replaced by the manure slurry in application. In the depth of 0.046 – 0.054 m, the initial NO_3^- content was assumed to be zero, and soil NO3- existed in the area beyond the central slurry area.

$$C_{NO3,s} = \frac{M_{NO3,s}\rho_b 10^{-3}(0.1 - z_2 + z_1)}{14(\int_0^{z1}\theta dz + \int_{z2}^{0.1}\theta dz)} \quad (53)$$

where $C_{NO3,s}$ is the dissolved NO_3^- content (mmol N/L), $M_{NO3,s}$ is the NO_3^- content (mg N/kg dw), ρ_b is the bulk density (g dw/L soil) along with a factor of 10^{-3} converting (g dw/L soil) to (kg dw/L soil), a conversion factor of 1/14 from mg N to mmol N, and the volumetric water content profile $\theta(z)$.

d. Particular organic matter (POC) in manure

The amount of manure POC applied was estimated as the difference between TOC and manure DOC, ca. 30.91 g C/m^2. We assumed manure POC was concentrated in the soil volume dominated by manure, within ca. 1 mm from the center to both sides (a length of 2 mm). The POC content per dry weight is calculated as

$$C_{POC,m} = \frac{M_{POC,m}}{10^3\rho_b({z_2}' - {z_1}')} \quad (54)$$

where $C_{POC,m}$ is the manure POC content (g C/g dw), $M_{POC,m}$is the amount of manure POC in application (g C/m^2), ρ_b is the bulk density (g dw/L soil) with a factor of 10^3 converting g dw/L soil to g dw/m^3 soil, and $({z_2}' - {z_1}')$ is the length of manure POC zone from 0.049 m to 0.051 m. Manure POC content is a piecewise function over depth, where the value is zero for $z<{z_1}'$ and $z>{z_2}'$ and non-zero for ${z_1}'<z<{z_2}'$ (${z_1}'$= 0.049 m, ${z_2}'$= 0.051 m).

e. NO_2^-

The initial NO_2^- content within the manure-treated soil profile was assumed to be zero.

f. Gases

Four components, CO_2, O_2, N_2O and N_2, in the model were considered in the gas phase. As we had no measurements for the initial gas concentrations, we considered the initial concentrations of the four components equivalent to the ambient atmospheric content at each sampling point while taking into account the exclusion of O_2 in hotspot volumes. The atmospheric N_2 and O_2 were considered to be 0.78 atm and 0.21 atm respectively. CO_2 and N_2O were considered to be 4.1×10^{-4} atm and 3.3×10^{-7} atm respectively (World Meteorological Organization, 2021). The gas concentration were calculated by the ideal gas equation:

$$C_{gas} = \frac{n}{V}\cdot 1000 = \frac{P_{gas}}{RT}\cdot 1000 \quad (55)$$

where C_{gas} is the gas concentration (mmol/L), n is the molar mass (mol) within a volume of air V (L), P_{gas} is the partial pressure of the individual gases (atm), R is a constant of 0.0821 L·atm/(mol·K), T is the temperature of 288.15 K, and 1000 is a conversion factor from mol/L to mmol/L.

The initial values of N_2, O_2, CO_2 and N_2O within the soil air were calculated to be 33.0 mmol/L, 8.9 mmol/L, 0.017 mmol/L, and 1.4×10^{-5} mmol/L. For the two sampling points (at the depths of 0.049 m and 0.051 m) most close to the center, we assumed the O_2 concentration to be zero.

S7. Parameters

S7.1 Diffusion coefficients

- Base diffusion coefficients

Base ion diffusion coefficients for most components refers to (Haynes, 2014) at 25 °C, and gas diffusion coefficients at 20 °C. For N_2O, diffusion coefficients at 15 °C were calculated according to (Massman, 1998).

Table S3. Base diffusion coefficients

Component	Phase	D (m^2/d)	Temperature	Reference
NO_2^-	water	1.65E-04	298.15	(Haynes, 2014)
NO_3^-	water	1.64E-04	298.15	(Haynes, 2014)
NH_4^+	water	1.69E-04	298.15	(Haynes, 2014)
DOC	water	8.38E-05	298.15	*
N_2O	air	1.37	288.15 K	(Massman, 1998)
N_2	air	1.75	293.15 K	(Haynes, 2014)
CO_2	air	1.31	293.15 K	(Haynes, 2014)
O_2	air	1.75	293.15 K	(Haynes, 2014)

*The value of DOC were calculated based on the mean value of diffusion coefficients of acetate, butyrate and propionate (Haynes, 2014). The three components are significant components of water-soluble C in the slurries (Paul and Beauchamp, 1989).

- Diffusion coefficients of liquid and gas at 15 °C (D_o)

The diffusion coefficients of DOC, NO_2^-, NO_3^- , and NH_4^+ in soil water were adjusted for temperature from the equation of Stokes-Einstein:

$$\frac{D_{T1}}{D_{T2}} = \frac{T_1}{T_2} \times \frac{\mu T_2}{\mu T_1}$$

The diffusion coefficients of N_2O, N_2, CO_2, and O_2 in soil air were adjusted for temperature (Gilliland, 1934):

$$\frac{D_{T1}}{D_{T2}} = (\frac{T_1}{T_2})^{1.5}$$

Table S4. Adjusted base diffusion coefficients at 15 °C (288.15 K)

Component	Phase	D_o (m^2/d)	Temperature
NO_2^-	water	1.25E-04	288.15 K
NO_3^-	water	1.24E-04	288.15 K
NH_4^+	water	1.28E-04	288.15 K
DOC	water	6.34E-05	288.15 K
N_2O	air	1.37	288.15 K
N_2	air	1.70	288.15 K
CO_2	air	1.35	288.15 K
O_2	air	1.70	288.15 K

- The effective diffusion coefficients were expressed as:

$$D_{\text{eff,aq}} = \theta_{aq}^3 D_{\text{o}} \quad \text{(in water phase)}$$

$$D_{\text{eff,g}} = \theta_{g}^{4/3} D_{\text{o}} \quad \text{(in gas phase)}$$

S7.2 Biotic parameters

In the model, the maximum potential reaction rate regarding the soil V_{max} (mmol/g dw/day) is expressed as μ_{max}*B, where μ_{max} (mmol/g biomass/day) is the maximum reaction rate regarding the microbial biomass, and B (g biomass/g dw) is the microbial biomass content in the -100 hPa soil. We determined the value ranges of V_{max} by looking at relevant experimental studies and then determined the value ranges of μ_{max} by dividing the V_{max} by the basal biomass of the involved microbes in the soil. μ_{max} was used as the model parameter and the relevant literature considered for V_{max} was shown in the sources and notes in Tables S5 and S6. The half-saturation constant for solute components represents the concentration in water (mmol/L water) and the half-saturation constant for gas components represents the concentration in air (mmol/L air).

Table S5. Parameters with fixed values in the model

Symbols	Descriptions	Units	Fixed values	Lower limits	Upper limits	Sources and notes
$k_{NH4\_NO2\_n}$	Half-saturation constant of NH_4^+ for NO_2^- production in nitrification	mmol/L	0.001	0.001	0.04	(Auyeung et al., 2015)

$k_{O2\_NO2\_n}$	Half-saturation constant of O_2 for NO_2^- production in nitrification	mmol/L	0.07	0.01	2	This study
$k_{O2\_NO3\_n}$	Half-saturation constant of O_2 for NO_3^- production in nitrification	mmol/L	0.1	0.01	3	This study
$k_{NH4\_N2O\_n}$	Half-saturation constant of NH_4^+ for N_2O production in nitrification	mmol/L	0.001	0.001	0.04	This study
$k_{O2\_N2O\_n}$	Half-saturation constant of O_2 for N_2O production in nitrification	mmol/L	0.07	0.01	2	This study
$k_{NH4\_N2O\_nd}$	Half-saturation constant of NH_4^+ for N_2O production in nitrifier denitrification	mmol/L	0.001	0.001	0.04	This study
$k_{O2\_N2O\_nd}$	Half-saturation constant of O_2 for N_2O production in nitrifier denitrification	mmol/L	0.01	0.01	2	This study
$k_{N2O\_N2\_dn}$	Half-saturation constant of N_2O for N_2 production in denitrification	mmol/L	5E-6	1E-06	0.001	(Betlach and Tiedje, 1981)
$k_{I\_NO2\_dn}$	Inhibition constant of O_2 for NO_2^- production in denitrification	mmol/L	0.1	0.01	2	This study
$k_{I\_N2O\_dn}$	Inhibition constant of O_2 for N_2O production in denitrification	mmol/L	0.04	0.01	2	This study
$k_{I\_N2O\_nd}$	Inhibition constant of O_2 for N_2O production in nitrifier denitrification	mmol/L	0.04	0.01	2	This study
$k_{I\_N2\_dn}$	Inhibition constant of O_2 for N_2 production in denitrification	mmol/L	0.04	0.01	2	This study

y_{AER}	Yield coefficient for aerobic bacteria	g C/g C	0.3	0.15	0.6	This study
y_{AOB}	Yield coefficient for AOB	g N/g N	0.013	0.007	0.026	(Chen et al., 2019)
y_{NOB}	Yield coefficient for NOB	g N/g N	0.004	0.002	0.008	(Chen et al., 2019)
y_{DEN}	Yield coefficient for denitrifiers	g C/g C	0.3	0.15	0.6	This study
a_{AER}	Decay rate for aerobic bacteria	1/day	0.1	0.05	0.2	This study
a_{AOB}	Decay rate for AOB	1/day	0.096	0.05	0.19	(Chen et al., 2019)
a_{NOB}	Decay rate for NOB	1/day	0.096	0.05	0.19	(Chen et al., 2019)
a_{DEN}	Decay rate for denitrifiers	1/day	0.1	0.05	0.2	This study
α_{SOC}	Decomposition rate of SOC	1/day	0.001	-	-	This study
α_{POC}	Decomposition rate of manure POC	1/day	0.01	-	-	This study
f_{Cbio}	C content in microbial biomass	g C/g biomass	0.53	-	-	(Khalil et al., 2005)
f_{Nbio}	N content in microbial biomass	g N/g biomass	0.066	-	-	This study

Note: blank values indicate the parameter value was not changed to check the sensitivity. The value of α_{SOC} was set as 0.001 1/day, so that the amount of degraded SOC following the first-order kinetics (6.57×10^4 mg C/m^2) was comparable to the cumulative CO_2-C emissions from control treatments (5.11×10^4 -5.26×10^4 mg C/m^2) during incubation. The value of α_{POC} took ten times the value of α_{SOC}. f_{Nbio} was estimated from f_{Cbio} by assuming a C/N ratio of 8.

Table S6. Parameters used in mode calibration and calibrated values.

Symbols	Descriptions	Units	Calibrated values	Lower limits	Upper limits	Sources and notes

$k_{C\_CO2\_r}$	Half-saturation constant of DOC for CO_2 production in aerobic respiration	mmol/L	4.07	0.5	10	This study
$k_{O2\_CO2\_r}$	Half-saturation constant of O_2 for CO_2 production in aerobic respiration	mmol/L	0.86	0.01	2	This study
$k_{NO2\_NO3\_n}$	Half-saturation constant of NO_2^- for NO_3^- production in nitrification	mmol/L	0.47	0.009	0.54	(Nowka et al., 2015)
$k_{NO2\_N2O\_nd}$	Half-saturation constant of NO_2^- for N_2O production in nitrifier denitrification	mmol/L	0.028	0.001	0.05	This study
$k_{NO3\_NO2\_dn}$	Half-saturation constant of NO_3^- for NO_2^- production in denitrification	mmol/L	3.50	0.001	3.5	(Betlach and Tiedje, 1981; Kohl et al., 1976)
$k_{C\_NO2\_dn}$	Half-saturation constant of DOC for NO_2^- production in denitrification	mmol/L	4.62	1	10	This study
$k_{NO2\_N2O\_dn}$	Half-saturation constant of NO_2^- for N_2O production in denitrification	mmol/L	0.001	0.001	0.05	(Betlach and Tiedje, 1981)
$k_{C\_N2O\_dn}$	Half-saturation constant of DOC for N_2O production in denitrification	mmol/L	8.10	0.5	10	This study
$k_{C\_N2\_dn}$	Half-saturation constant of DOC for	mmol/L	0.5	0.5	10	This study

	N_2 production in denitrification					
μ_{CO2_r}	Maximum velocity for CO_2 production in aerobic respiration	mmol CO_2 produced/g biomass/day	202.8	3.78	1889.76	(Eberwein et al., 2015)
μ_{NO2_n}	Maximum velocity for NO_2^- production in nitrification	mmol NO_2^- produced/g biomass/day	115.2	11.34	160.00	(Højberg et al., 1996)
μ_{NO3_n}	Maximum velocity for NO_3^- production in nitrification	mmol NO_3^- produced/g biomass/day	159.6	11.34	160.00	(Højberg et al., 1996)
μ_{N2O_n}	Maximum velocity for N_2O production in nitrification	mmol N_2O produced/g biomass/day	1.89	1.89	75.59	This study
μ_{N2O_nd}	Maximum velocity for N_2O production in nitrifier denitrification	mmol N_2O produced/g biomass/day	12	1.89	75.59	This study
μ_{NO2_dn}	Maximum velocity for NO_2^- production in denitrification	mmol NO_2^- produced/g biomass/day	100	15.00	302.36	(Højberg et al., 1996)
μ_{N2O_dn}	Maximum velocity for N_2O production in denitrification	mmol N_2O produced/g biomass/day	45.8	1.89	75.59	(Holtan-Hartwig et al., 2000; Tiedje et al., 1982)
μ_{N2_dn}	Maximum velocity for N_2 production in denitrification	mmol N_2 produced/g biomass/day	48.7	1.89	75.59	(Højberg et al., 1996)

S7.3 Sensitivity analysis

We conducted a local sensitivity analysis based on the baseline simulation where each parameter values was increased by 20 % one at time and the influence on cumulative gas emissions was quantified by the sensitivity index (S_θ). The results are shown in Fig. S24.

$$S_\theta = \frac{\Delta y / y}{\Delta \theta / \theta}$$

Where θ and y are the parameter and the affected variable; $\Delta\theta$ and Δy are the changes of the parameter and the variable respectively.

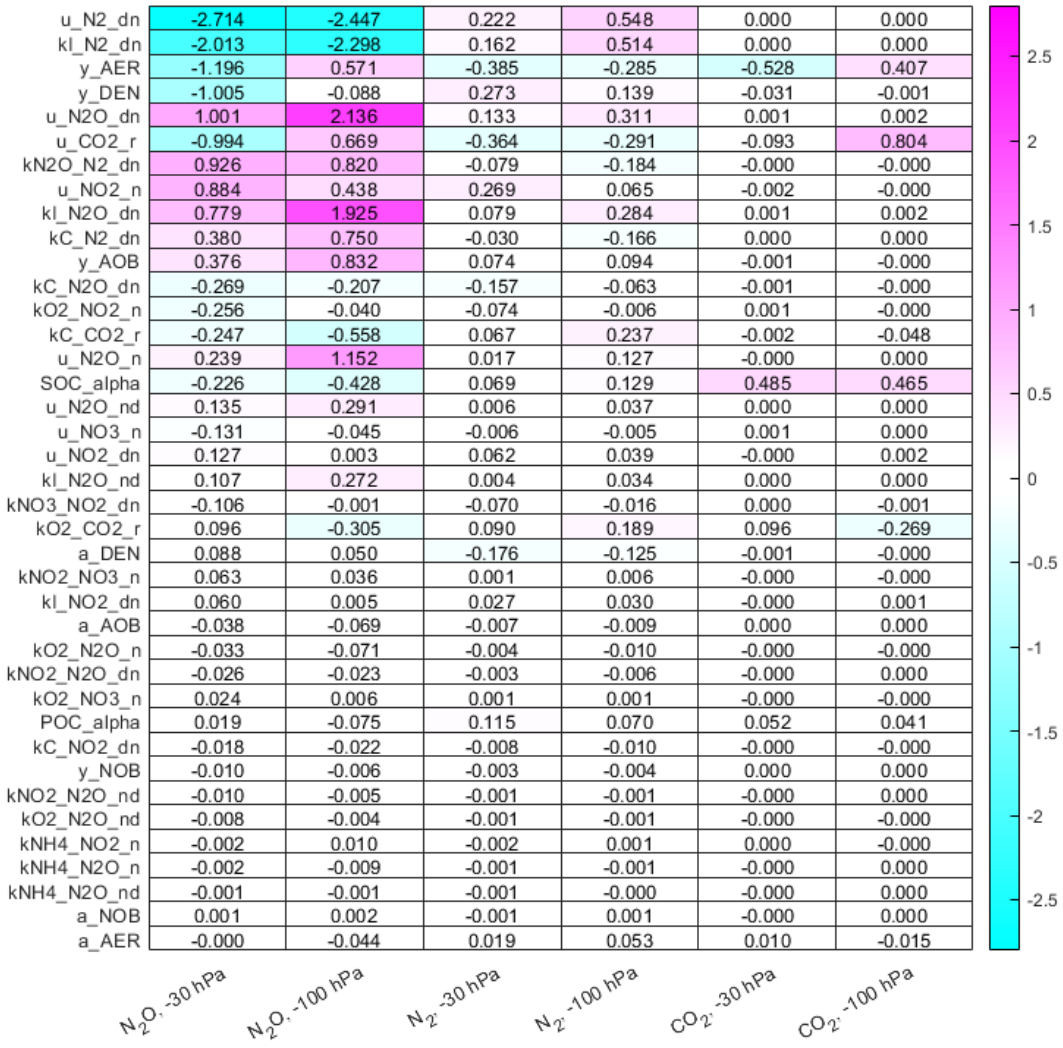

Figure S24. The sensitivity index of parameters regarding cumulative gas emissions in two soil moisture conditions.

S7.4 Parameter correlation

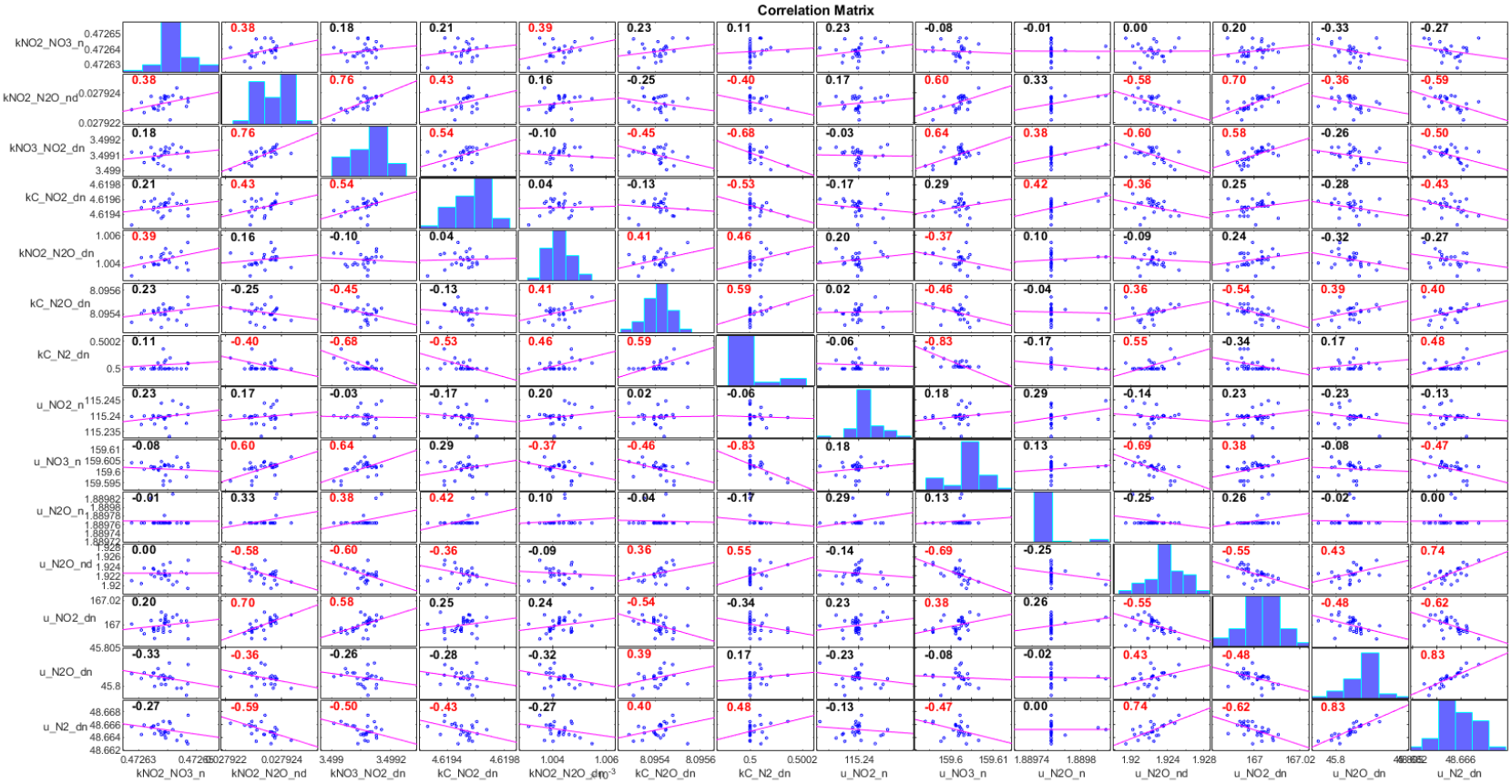
Correlation Matrix
kNO2_NO3_n
kNO2_N2O_nd
kNO3_NO2_dn
kC_NO2_dn
kNO2_N2O_dn
kC_N2O_dn
kC_N2_dn
u_NO2_n
u_NO3_n
u_N2O_n
u_N2O_nd
u_NO2_dn
u_N2O_dn
u_N2_dn

Figure S25. Correlation plot between parameters in the posterior ensemble of 1 % the best runs (33 runs). Red color indicates correlations are significantly different from zero.

S8. Model statistics

Table S7. Model evaluation statistics for gas emissions. Relative ME_{cum} indicates the relative mean error of cumulative gas fluxes where the cumulative gas fluxes were calculated by trapezoidal integration over the sampling days. R^2 is the coefficient of determination. R^2 was not calculated for N_2 fluxes at -100 hPa, as only two sampling values were valid.

	N_2O, -30 hPa	N_2O, -100 hPa	N_2, -30 hPa	N_2, -100 hPa	CO_2, -30 hPa	CO_2, -100 hPa
relative RMSE	1.45	11.2	0.65	3.56	0.62	0.45
relative ME_{cum}	0.19	0.93	-0.29	3.54	-0.31	-0.40
R^2	0.43	0.71	0.47	-	0.07	0.84

References

Auyeung, D. S. N., Martiny, J. B. H. and Dukes, J. S.: Nitrification kinetics and ammonia-oxidizing community respond to warming and altered precipitation, Ecosphere, 6, 1–17, doi:10.1890/ES14-00481.1, 2015.

Betlach, M. R. and Tiedje, J. M.: Kinetic explanation for accumulation of nitrite, nitric oxide, and nitrous oxide during bacterial denitrification, Appl. Environ. Microbiol., 42, 1074–1084, doi:10.1128/aem.42.6.1074-1084.1981, 1981.

Chen, X., Ni, B. J. and Sin, G.: Nitrous oxide production in autotrophic nitrogen removal granular sludge: a modeling study, Biotechnol. Bioeng., 116, 1280–1291, doi:10.1002/bit.26937, 2019.

Davidson, E. A., Samanta, S., Caramori, S. S. and Savage, K.: The Dual Arrhenius and Michaelis – Menten kinetics model for decomposition of soil organic matter at hourly to seasonal time scales, Glob. Chang. Biol., 18, 371–384, doi:10.1111/j.1365-2486.2011.02546.x, 2012.

Eberwein, J. R., Oikawa, P. Y., Allsman, L. A. and Jenerette, G. D.: Carbon availability regulates soil respiration response to nitrogen and temperature, Soil Biol. Biochem., 88, 158–164, doi:10.1016/J.SOILBIO.2015.05.014, 2015.

Gilliland, E. R.: Diffusion coefficients in gaseous systems, Ind. Eng. Chem., 26, 681–685, doi:10.1021/IE50294A020/ASSET/IE50294A020.FP.PNG_V03, 1934.

Gjettermann, B., Styczen, M., Hansen, H. C. B., Vinther, F. P. and Hansen, S.: Challenges in modelling dissolved organic matter dynamics in agricultural soil using DAISY, Soil Biol. Biochem., 40, 1506–1518, doi:10.1016/J.SOILBIO.2008.01.005, 2008.

Haynes, W. M.: CRC handbook of chemistry and physics, CRC press., 2014.

Højberg, O., Binnerup, S. J. and Sørensen, J.: Potential rates of ammonium oxidation, nitrite oxidation, nitrate reduction and denitrification in the young barley rhizosphere, Soil Biol. Biochem., 28, 47–54, doi:10.1016/0038-

0717(95)00119-0, 1996.
Holtan-Hartwig, L., Dörsch, P. and Bakken, L. R.: Comparison of denitrifying communities in organic soils: kinetics of NO_3^- and N_2O reduction, Soil Biol. Biochem., 32, 833–843, doi:10.1016/S0038-0717(99)00213-8, 2000.
Jensen, J. L., Christensen, B. T., Schjønning, P., Watts, C. W. and Munkholm, L. J.: Converting loss-on-ignition to organic carbon content in arable topsoil: pitfalls and proposed procedure, Eur. J. Soil Sci., 69, 604–612, doi:10.1111/EJSS.12558, 2018.
Khalil, K., Renault, P., Guerin, N. and Mary, B.: Modelling denitrification including the dynamics of denitrifiers and their progressive ability to reduce nitrous oxide: comparison with batch experiments, Eur. J. Soil Sci., 56, 491–504, doi:10.1111/j.1365-2389.2004.00681.x, 2005.
Kohl, D. H., Vithayathil, F., Whitlow, P., Shearer, G. and Chien, S. H.: Denitrification kinetics in soil systems: the significance of good fits of data to mathematical forms, Soil Sci. Soc. Am. J., 40, 249–253, doi:10.2136/sssaj1976.03615995004000020018x, 1976.
Massman, W. J.: A review of the molecular diffusivities of H_2O, CO_2, CH_4, CO, O_3, SO_2, NH_3, N_2O, NO, and NO_2 in air, O_2 and N_2 near STP, in Atmospheric Environment, vol. 32, pp. 1111–1127, Pergamon., 1998.
Millington, R. J.: Gas diffusion in porous media, Science (80-.)., 130, 100–102, doi:10.1126/science.130.3367.100.b, 1959.
Nowka, B., Daims, H. and Spieck, E.: Comparison of oxidation kinetics of nitrite-oxidizing bacteria: Nitrite availability as a key factor in niche differentiation, Appl. Environ. Microbiol., 81, 745–753, doi:10.1128/AEM.02734-14, 2015.
Olesen, T., Moldrup, P. and Gamst, J.: Solute diffusion and adsorption in six soils along a soil texture gradient, Soil Sci. Soc. Am. J., 63, 519–524, doi:10.2136/sssaj1999.03615995006300030014x, 1999.
Paul, J. W. and Beauchamp, E. G.: Effect of carbon constituents in manure on denitrification in soil, Can. J. Soil Sci., 69, 49–61, doi:10.4141/cjss89-006, 1989.
Petersen, S. O., Nielsen, T. H., Frostegård, Å. and Olesen, T.: O_2 uptake, C metabolism and denitrification associated with manure hot-spots, Soil Biol. Biochem., 28, 341–349, doi:10.1016/0038-0717(95)00150-6, 1996.
Petersen, S. O., Olsen, A. B., Elsgaard, L., Triolo, J. M. and Sommer, S. G.: Estimation of methane emissions from slurry pits below pig and cattle confinements, PLoS One, 11, 1–16, doi:10.1371/journal.pone.0160968, 2016.
Tiedje, J. M., Sexstone, A. J., Myrold, D. D., Robinson, J. A. and Denitrifica, J. A.: Denitrification: ecological niches, competition and survival I, Antonie Van Leeuwenhoek, 48, 569–583, 1982.
World Meteorological Organization: WMO Greenhouse gas bulletin: the state of greenhouse gases in the atmosphere based on global observations through 2020, [online] Available from: https://library.wmo.int/index.php?lvl=notice_display&id=21975#.YgFFTrrMJaQ (Accessed 7 February 2022), 2021.